Progress In Electromagnetics Research Letters, Vol. 50, 73–77, 2014

Electromagnetic Characterization of Anisotropic and Weakly Conductive Materials by Using Resonant Circuits

Hocine Menana*

Abstract—This work deals with the electromagnetic characterization of the electrical conductivity of anisotropic and weakly conductive materials by using resonant circuits. Experimental results characterizing a carbon fiber reinforced polymer (CFRP) ply are presented.

1. INTRODUCTION

In order to evaluate physical and geometrical properties or to detect and characterize defects in conductive materials, the eddy current nondestructive testing is widely used [1, 2]. However, this method is less efficient for weakly conductive materials, such as carbon fiber reinforced polymers (CFRPs) [3–5]. To get significant signals, higher frequencies must be used which is followed by undesirable capacitive effects [5]. For such materials, the use of resonant circuits is an interesting alternative [6]. Indeed, in this case, the impact of the impedance variation on the resonant frequency is more significant than the impedance variation itself. In this work, we present some experimental results dealing with the characterization of CFRPs conductivity by using resonant circuits. The experimental setup is described in the next section, and experimental results are presented and discussed in the last section.

2. THE EXPERIMENTAL SETUP

An impedance analyzer (AGILENT 4294A) is used to measure the variations of the real and the imaginary parts of the impedance of a coil wound on a ferrite torus containing an air-gap in which a CFRP ply is inserted. Figure 1 gives the physical and schematic views of the experimental setup. The CFRP ply is constituted of carbon fibers embedded in an electrically nonconductive matrix. It is characterized by an anisotropic electrical conductivity given by (1), where σ_L and σ_T denote the electrical conductivities in the directions parallel and transverse to the carbon fibers. Notice that the CFRPs present high anisotropies ($\sigma_L \gg \sigma_T$) [7].

$$\bar{\bar{\sigma}} = \begin{bmatrix} \sigma_L & 0 & 0 \\ 0 & \sigma_T & 0 \\ 0 & 0 & \sigma_T \end{bmatrix} \tag{1}$$

The numerical values of the system parameters are given in Table 1. To deal with the CFRP ply anisotropy, the width of the torus (τ) is chosen to be much greater than its thickness ($(R_e - R_i)/2$). In fact, the latter has to be as small as possible.

Received 30 October 2014, Accepted 17 November 2014, Scheduled 4 December 2014
* Corresponding author: Hocine Menana (hocine.menana@ecole-navale.fr).
The author is with the French Naval Academy Research Institute (IRENAv), Brest, France.

Table 1. Numerical values of the system parameters.

Parameter	Numerical value
Ferrite torus	
Ferrite type	4W1500
Inner radius (R_i)	9 mm
Outer radius (R_e)	14 mm
Width (τ)	28.5 mm
Relative permeability (μ_r)	252 at 100 kHz
Air-gap (e)	0.59 mm
Coil	
Material	Copper insulated (0.2 mm Ø)
Number of turns	250
CFRP ply	
Thickness (δp)	0.125 mm
Electrical conductivities (σ_L and σ_T)	Unknowns ($\sigma_L \gg \sigma_T$)

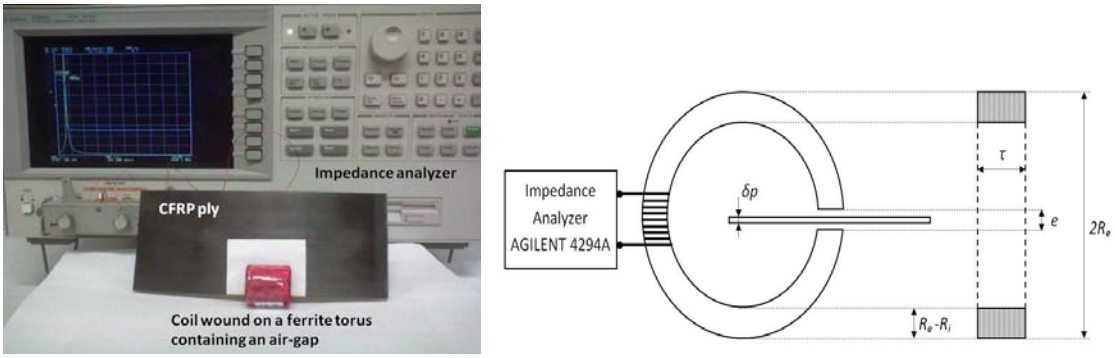

Figure 1. The experimental setup.

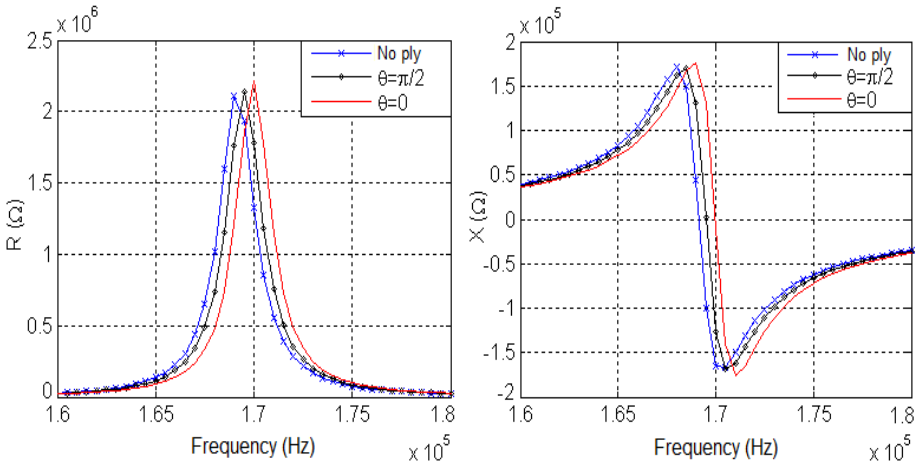

Figure 2. Variation of the real (R) and imaginary (X) parts of the coil impedance as function of the fibers orientation in the torus air-gap.

3. RESULTS AND DISCUSSION

Figure 2 shows the variations of the real and imaginary parts of the coil impedance ($Z = R + jX$) according to the frequency, for three cases. In the first one (No ply), no CFRP ply is present in the

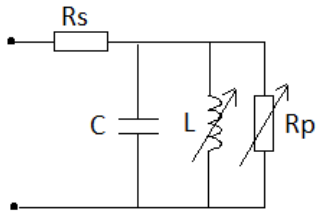

Figure 3. The equivalent electrical circuit of the system.

torus air-gap, and in the two other cases, the CFRP ply is placed in the torus air-gap, with the fibers oriented in the directions parallel ($\theta = 0$) ant transverse ($\theta = \pi/2$) to the direction of the torus width (τ). We notice that the resonant frequency and the real part of the coil impedance increase with the electrical conductivity (linked to the fibers orientation in the torus air-gap). For any further use, Table A1 gives the measurements numerical data.

Neglecting the magnetic flux leakage in the coil and the capacitive coupling between the fibers in the CFRP ply, the system can be modeled by the electrical circuit given in Figure 3. The series resistance, R_s, represents the resistive losses in the coil conductors. The parallel capacitance, C, is the equivalent capacitance between the coil turns, and the parallel resistance R_p, represents the losses in the ferrite core and in the CFRP ply. The inductance, L, is the coil inductance taking account of the mutual inductance with the CFRP ply. The series resistance and capacitance are assumed to be constant, while the inductance and the parallel resistance vary with the frequency. The eddy currents in the ply create a magnetic field that opposes the magnetic fields created by the coil. This leads to a decrease of circuit inductance and thus an increase of the resonant frequency given as follows:

$$f_0 = \left(2\pi\sqrt{LC}\right)^{-1} \tag{2}$$

According to the electrical model given in Figure 3, at the resonant frequency ($C\omega_0 = L^{-1}\omega_0^{-1}$), we have:

$$Z_{f=f_0} = R_s + R_p \tag{3}$$

Neglecting the variation of the losses in the ferrite core (resonant frequencies close to each other), and considering the capacitance, C, as a constant, from (2) and (3), we extract the variations of the system resistance and inductance, due to the eddy currents in the ply which depend directly on the electrical conductivity (resistivity) of the latter. The relation between the resistance variation and the electrical conductivity of the tested material depends on the eddy currents distribution in the latter, which can be obtained by numerical modeling [8].

Four parameters can be used to characterize the CFPR ply anisotropic conductivity. These parameters correspond to the variations the resistance and the inductance for both situations where the fibers are parallel and transverse to the direction of the torus width (τ). This would permit to distinguish between the parallel and transverse conductivity. Indeed, if the resistance variation would be the same for any two couples of the longitudinal and transversal conductivities (σ_{1_L}, σ_{1_T}) and (σ_{2_L}, σ_{2_T}), the inductance variation would be different since the eddy currents repartition would be different.

4. CONCLUSION

This work aims to show the possibility to characterize low conductive and anisotropic material by using resonant circuits. Indeed, in this case, the effect of the impedance variation (i.e., the variation of the resonant frequency) is more significant that the impedance variation itself. The resistance and inductance variations are directly obtained from the measurements. A numerical modeling is however necessary to determine the eddy currents repartition in the tested sample, and thus the relation between the measured parameters and the electrical conductivity of the latter. The use of both the resistance and inductance variations corresponding to the fibers orientations parallel and transverse to the torus width would permit to distinguish between the longitudinal and transversal conductivities of a CFRP ply. For isotropic materials, the use of a ferrite torus of a circular section would simplify the problem.

ACKNOWLEDGMENT

Work done in part at the IREENA research institute (Saint Nazaire — France).

APPENDIX A.

Table A1. Measurements numerical data.

Frequency	**Real part of the impedance (Ω)**			**Imaginary part of the impedance (Ω)**		
(Hz)	No ply	$\Theta = 0$	$\Theta = \pi/2$	No ply	$\Theta = 0$	$\Theta = \pi/2$
$1.600e+05$	$2.786148e+04$	$2.279917e+04$	$2.586576e+04$	$2.450074e-01$	$2.263570e-01$	$2.363080e-01$
$1.605e+05$	$3.132445e+04$	$2.534159e+04$	$2.891973e+04$	$2.583648e-01$	$2.376523e-01$	$2.487339e-01$
$1.610e+05$	$3.537203e+04$	$2.835689e+04$	$3.265066e+04$	$2.732941e-01$	$2.502069e-01$	$2.625271e-01$
$1.615e+05$	$4.028503e+04$	$3.203362e+04$	$3.695212e+04$	$2.900719e-01$	$2.641532e-01$	$2.779249e-01$
$1.620e+05$	$4.620950e+04$	$3.626074e+04$	$4.208319e+04$	$3.090422e-01$	$2.797416e-01$	$2.951983e-01$
$1.625e+05$	$5.346788e+04$	$4.136605e+04$	$4.837182e+04$	$3.306342e-01$	$2.972794e-01$	$3.148166e-01$
$1.630e+05$	$6.255148e+04$	$4.761049e+04$	$5.612466e+04$	$3.555064e-01$	$3.172081e-01$	$3.372083e-01$
$1.635e+05$	$7.407781e+04$	$5.527677e+04$	$6.586814e+04$	$3.842890e-01$	$3.399969e-01$	$3.630182e-01$
$1.640e+05$	$8.891522e+04$	$6.491503e+04$	$7.824975e+04$	$4.180613e-01$	$3.661961e-01$	$3.930184e-01$
$1.645e+05$	$1.085930e+05$	$7.719180e+04$	$9.426756e+04$	$4.579700e-01$	$3.967451e-01$	$4.281947e-01$
$1.650e+05$	$1.352394e+05$	$9.322669e+04$	$1.157065e+05$	$5.057709e-01$	$4.327691e-01$	$4.700445e-01$
$1.655e+05$	$1.726188e+05$	$1.146660e+05$	$1.447556e+05$	$5.639791e-01$	$4.756061e-01$	$5.201916e-01$
$1.660e+05$	$2.266346e+05$	$1.438437e+05$	$1.860166e+05$	$6.350389e-01$	$5.271118e-01$	$5.813420e-01$
$1.665e+05$	$3.080841e+05$	$1.831984e+05$	$2.461872e+05$	$7.218251e-01$	$5.872666e-01$	$6.560262e-01$
$1.670e+05$	$4.377328e+05$	$2.393007e+05$	$3.385892e+05$	$8.266323e-01$	$6.597830e-01$	$7.476082e-01$
$1.675e+05$	$6.533585e+05$	$3.282188e+05$	$4.869948e+05$	$9.404559e-01$	$7.526277e-01$	$8.555484e-01$
$1.680e+05$	$1.021813e+06$	$4.778234e+05$	$7.365739e+05$	$1.016488e+00$	$8.682847e-01$	$9.660364e-01$
$1.685e+05$	$1.593530e+06$	$7.413962e+05$	$1.157756e+06$	$8.862069e-01$	$9.922571e-01$	$1.010477e+00$
$1.690e+05$	$2.107978e+06$	$1.207445e+06$	$1.761497e+06$	$2.580158e-01$	$1.044041e+00$	$7.711258e-01$
$1.695e+05$	$1.932922e+06$	$1.858742e+06$	$2.136929e+06$	$-5.914435e-01$	$7.716848e-01$	$1.792905e-02$
$1.700e+05$	$1.329456e+06$	$2.216272e+06$	$1.782632e+06$	$-9.692054e-01$	$-5.968003e-02$	$-7.418268e-01$
$1.705e+05$	$8.495602e+05$	$1.778558e+06$	$1.183590e+06$	$-9.744539e-01$	$-8.229365e-01$	$-9.883183e-01$
$1.710e+05$	$5.587350e+05$	$1.148404e+06$	$7.593155e+05$	$-8.715187e-01$	$-1.028439e+00$	$-9.492807e-01$
$1.715e+05$	$3.866824e+05$	$7.279928e+05$	$5.066795e+05$	$-7.610862e-01$	$-9.638596e-01$	$-8.404616e-01$
$1.720e+05$	$2.819335e+05$	$4.841161e+05$	$3.556730e+05$	$-6.664162e-01$	$-8.444544e-01$	$-7.334281e-01$
$1.725e+05$	$2.140921e+05$	$3.392570e+05$	$2.609388e+05$	$-5.891854e-01$	$-7.333779e-01$	$-6.423452e-01$
$1.730e+05$	$1.673428e+05$	$2.491819e+05$	$1.987708e+05$	$-5.252169e-01$	$-6.411812e-01$	$-5.677289e-01$
$1.735e+05$	$1.337312e+05$	$1.900224e+05$	$1.559866e+05$	$-4.717878e-01$	$-5.663341e-01$	$-5.068411e-01$
$1.740e+05$	$1.090573e+05$	$1.495824e+05$	$1.256258e+05$	$-4.272479e-01$	$-5.053883e-01$	$-4.565211e-01$
$1.745e+05$	$9.055716e+04$	$1.205666e+05$	$1.032829e+05$	$-3.895879e-01$	$-4.554870e-01$	$-4.148057e-01$
$1.750e+05$	$7.626812e+04$	$9.926991e+04$	$8.639984e+04$	$-3.576831e-01$	$-4.139014e-01$	$-3.794927e-01$
$1.755e+05$	$6.525773e+04$	$8.310978e+04$	$7.334125e+04$	$-3.303572e-01$	$-3.788803e-01$	$-3.495590e-01$
$1.760e+05$	$5.642341e+04$	$7.059203e+04$	$6.307202e+04$	$-3.067705e-01$	$-3.490107e-01$	$-3.237659e-01$
$1.765e+05$	$4.937061e+04$	$6.076528e+04$	$5.485723e+04$	$-2.863461e-01$	$-3.232969e-01$	$-3.013883e-01$
$1.770e+05$	$4.360819e+04$	$5.281188e+04$	$4.811773e+04$	$-2.685212e-01$	$-3.010115e-01$	$-2.818049e-01$
$1.775e+05$	$3.882180e+04$	$4.637853e+04$	$4.260256e+04$	$-2.527575e-01$	$-2.814538e-01$	$-2.645274e-01$
$1.780e+05$	$3.477339e+04$	$4.105147e+04$	$3.797080e+04$	$-2.385479e-01$	$-2.642143e-01$	$-2.491608e-01$
$1.785e+05$	$3.132777e+04$	$3.661184e+04$	$3.408020e+04$	$-2.258276e-01$	$-2.488735e-01$	$-2.354017e-01$

Frequency	**Real part of the impedance (Ω)**			**Imaginary part of the impedance (Ω)**		
(Hz)	No ply	$\Theta = 0$	$\Theta = \pi/2$	No ply	$\Theta = 0$	$\Theta = \pi/2$
$1.790e+05$	$2.838513e+04$	$3.286697e+04$	$3.074988e+04$	$-2.143937e-01$	$-2.351427e-01$	$-2.230176e-01$
$1.795e+05$	$2.586727e+04$	$2.967811e+04$	$2.789270e+04$	$-2.039934e-01$	$-2.228309e-01$	$-2.117942e-01$
$1.800e+05$	$2.365945e+04$	$2.694047e+04$	$2.545031e+04$	$-1.945174e-01$	$-2.116914e-01$	$-2.016360e-01$

REFERENCES

1. Bore, T., P.-Y. Joubert, and D. Placko, "A differential DPSM based modeling applied to eddy current imaging problems," *Progress In Electromagnetics Research*, Vol. 148, 209–221, 2014.
2. Musolino, A., R. Rizzo, and E. Tripodi, "A quasi-analytical model for remote field eddy current inspection," *Progress In Electromagnetics Research M*, Vol. 26, 237–249, 2012.
3. Menana, H. and M. Féliachi, "Electromagnetic Characterization of the CFRPs anisotropic conductivity: Modeling and measurements," *Eur. Phys. J. Appl. Phys.*, Vol. 53, 21101, 2011.
4. Mook, G., R. Lange, and O. Koeser, "Non-destructive characterization of carbon-fiber-reinforced plastics by means of eddy-currents," *Composites Science and Technology*, Vol. 61, 865–873, 2001.
5. Menana, H. and M. Féliachi, "Modeling the response of a rotating eddy current sensor for the characterization of carbon fiber reinforced composites," *Eur. Phys. J. Appl. Phys.*, Vol. 52, 23304, 2010.
6. Xu, S., L. Yang, L. Huang, and H. S. Chen, "Experimental measurement method to determine the permittivity of extra thin materials using resonant metamaterials," *Progress In Electromagnetics Research*, Vol. 120, 327–337, 2011.
7. Pratap, S. B. and W. F. Weldon, "Eddy current in anisotropic composites applied to pulsed machinery," *IEEE Transactions on Magnetics*, Vol. 32, No. 2, 437–444, Mar. 1996.
8. Menana, H. and M. Féliachi, "An integro-differential model for 3D Eddy current computation in CFRPs," *IEEE Transactions on Magnetics*, Vol. 47, No. 4, 756–763, Apr. 2011.